



OPEN ACCESS

EDITED BY

Jiadong Qiu,
University of South China, China

REVIEWED BY

Nahla Hilal,
University of Fallujah, Iraq
Chendi Min,
Hunan University of Science and
Technology, China
Jie Ren,
Inner Mongolia University of
Technology, China

*CORRESPONDENCE

Lizhen Xu,
✉ 23203226081@stu.xust.edu.cn

RECEIVED 24 January 2025

ACCEPTED 14 July 2025

PUBLISHED 30 July 2025

CITATION

Wu Z, Xu L, Xin C and Zhang W (2025) Analysis
of the physical and mechanical properties of
coal-based solid waste filling material at early
ages.

Front. Mater. 12:1566391.

doi: 10.3389/fmats.2025.1566391

COPYRIGHT

© 2025 Wu, Xu, Xin and Zhang. This is an
open-access article distributed under the
terms of the [Creative Commons Attribution
License \(CC BY\)](#). The use, distribution or
reproduction in other forums is permitted,
provided the original author(s) and the
copyright owner(s) are credited and that the
original publication in this journal is cited, in
accordance with accepted academic practice.
No use, distribution or reproduction is
permitted which does not comply with
these terms.

Analysis of the physical and mechanical properties of coal-based solid waste filling material at early ages

Zheng Wu^{1,2}, Lizhen Xu^{1*}, Chang Xin¹ and Wen Zhang¹

¹School of Energy, Xi'an University of Science and Technology, Xi'an, China, ²Key Laboratory of Department of Education of Western Mine Mining and Disaster Prevention, Xi'an University of Science and Technology, Xi'an, China

Fly ash-based filling materials are widely used in coal mine backfilling due to their cost-effectiveness and environmental benefits, but their application is often hindered by low early-age strength, poor fluidity, and severe water segregation. This study aims to enhance the performance of such materials by examining the effects of varying water-to-binder ratios and fly ash contents on their early-age physical and mechanical properties. Five different mix proportions composed of cement, fly ash, and coal gangue were prepared and tested. Uniaxial compressive strength, elastic modulus, and porosity were measured over a 12–48 h curing period, and hydration characteristics were analyzed using XRD and SEM techniques. Results show that reducing fly ash content from 75% to 50% increases the 48-h uniaxial compressive strength and elastic modulus by 3.06 and 6.80 times, respectively, due to improved hydration kinetics and microstructural compactness. Furthermore, incorporating early-strength additives further enhances mechanical performance. These findings suggest that a mix with 50% fly ash and a water-to-binder ratio of 0.63 achieves optimal early-age strength and compactness, providing a practical solution for improving the performance and applicability of coal-based solid waste filling materials in mine backfilling operations.

KEYWORDS

fly ash-based filling material, early age, porosity, physical and mechanical properties, hydration process

1 Introduction

During the process of coal mining and utilization, a large amount of coal-based associated minerals and intermediate solid wastes—such as coal gangue, fly ash, and coal gasification slag—are generated. Among them, coal gangue accounts for 10%–15% of the total coal production (Li and Wang, 2019), and the accumulation of fly ash in China has approached 4 billion tons, with an annual increase of 600 million tons (Yang YX. et al., 2021; Jiang, 2020). With the continuous intensification of environmental protection efforts, mines undergo continuous mine filling and repair during and after mining operations. Preparing low-strength, low-cost underground filling materials using coal-based

solid waste like coal gangue and fly ash is a crucial approach for rapidly addressing ecological issues of coal mining and scientifically managing coal-based solid waste.

The coal mine filling technology is a technique that injects filling materials (such as coal gangue, fly ash, and cementitious materials) into the mined-out area to support the surrounding rock and reduce the deformation of the strata. It can not only reduce the impact of coal gangue discharge on the ground but also control the influence range of mining-induced subsidence through different filling positions and provide feasible solutions for the recovery of regional irregularities or replacement coal pillars and other coal resources. Thus, it controls the movement law of overlying strata and reduces the damage to the surface ecology. Therefore, the research on coal mine filling is of great significance.

The early strength of filling materials determines whether they can support the collapse of the goaf, thus affecting the coal yield. Recent studies have further emphasized the importance of early mechanical performance in fractured and dynamically loaded systems, such as Zhang et al. (2025), who investigated strength recovery in post-peak grouting of fragmented rock masses, and Lai et al. (2025), who analyzed the staged energy evolution in modified high-energy storage rock. Developing high-performance mine filling materials based on entirely solid waste or a high mass fraction of coal-based solid waste has become a trend (Peng and Bi, 2020; Liang et al., 2023). Qiu et al. (2025) and Zhou et al. (2025) have demonstrated, using particle-based and BPM-DFN models, that fracture evolution and rate-dependent tensile behavior are critical to understanding early-stage backfill integrity. The principal mechanism involves using gangue as aggregate and fly ash, activated gasification fine slag, and other latent pozzolans as cementitious materials. A small amount of cement clinker is added to provide an alkaline environment and a calcium source. The active substances like SiO_2 and Al_2O_3 in fly ash react with Ca(OH)_2 produced by cement hydration, triggering a secondary pozzolanic reaction that generates silicoaluminate gel, providing system strength. Yang et al. (2022) and Yang K. et al. (2021) determined through response surface methodology and regression fitting that the optimal ratios for filling materials based on coal-based solid waste such as desulfurized gypsum, gasification slag, and bottom ash are 0.2, 0.1, and 0.1, respectively. Their study also indicated that the compressive strength of the filling body made from these solid wastes significantly decreases at 28 days of curing compared to that at 7 days. Yang et al. (2017) prepared a new filling material using fly ash and coal gangue as the foundation, combined with lime and cement. The fly ash content could reach up to 79.2%, suggesting that appropriate amounts of lime and cement are beneficial for activating fly ash but may adversely affect the strength and bleeding of the filling material. Yu (2017) fully utilized solid waste from mining areas and power plants to prepare a new type of cementitious material and studied its strength and transport characteristics. The optimal ratio of cement: lime: desulfurization gypsum: fly ash was found to be 20%: 1.8%: 9%: 69.2% for the new coal mine cementitious material without the addition of activators.

Currently, most research on the physical properties of concrete focuses on the slow compression characteristics of hardened concrete, and studies on early-age physical properties are inadequate, especially for high-volume fly ash concrete (HVFAC). Existing research on the mechanical properties of fly ash concrete

primarily concentrates on standard fly ash content. Compared to standard fly ash concrete, HVFAC undergoes significant changes in its hydration process and internal structure, resulting in substantial differences in performance characteristics (Yu, 2017; Charpin et al., 2018). It is widely believed that the paste in concrete is a significant contributor to the time-varying development of its early physical and mechanical properties. In particular, the development of strength and stiffness in C–S–H gel within the paste is one of the essential factors influencing the physical and mechanical properties of concrete during its early stages (Huynh et al., 2018; Park and Choi, 2021; Wyrz et al., 2019). The incorporation of a large amount of fly ash directly affects the time-varying pattern of C–S–H gel strength and stiffness in hardened cement paste, further impacting the mechanical properties of concrete (Mallick et al., 2019; Yao et al., 2023; Ni, 2020). Differences in the hydration process of cement paste directly influence the development of parameters like maximum indentation depth and hardness (Zhou et al., 2011; Chen et al., 2019; Lavergne and Barthelemy, 2020). The physical and mechanical characteristics of cement-based paste materials can be controlled by these parameters. However, there is limited research on the impact of the early physical and mechanical properties of the paste on the development of HVFAC filling effects. Zhang et al. (2023) conducted research on the mechanical properties and damage evolution laws of multi-source coal-based solid waste cemented backfill (CBSWCB) through uniaxial compression tests, acoustic emission (AE) response analysis, and microstructure characterization. So et al. (2023) discussed a summary of the common methods for coal upgrading to prepare more suitable precursors for the production of graphene-related materials (GRMs). They also compiled and analyzed the reported routes and methods for preparing GRMs from coal and coal derivatives. Additionally, they discussed the potential applications of coal-based GRMs. Qiu et al. (2025) and Zhou et al. (2025) studied the damage evolution process under complex stress conditions using rock mechanics testing methods.

Despite the extensive research on coal-based solid waste filling materials, critical gaps remain in understanding the early-age physical and mechanical properties of these materials. Previous studies have primarily focused on long-term strength development (e.g., 28-day curing) while neglecting the time-sensitive evolution of microstructure and mechanical performance during the initial 48 h, a period crucial for ensuring goaf stability in mining operations. Moreover, existing investigations into HVFAC often overlook the dynamic interplay between the fly ash content, water-to-binder ratio, and early-age hydration kinetics, leading to suboptimal mix designs that compromise both strength and workability. To address these limitations, this study systematically investigates the real-time hydration process, porosity evolution, and mechanical behavior of fly ash–gangue backfill materials under five distinct mixing ratios, with a focus on the critical 12–48 h window. By correlating microstructural changes with macroscopic properties, we reveal how reducing the fly ash content from 75% to 50% enhances early-age strength by 3.06-fold—a finding that challenges conventional high-fly-ash formulations. This research not only provides a theoretical basis for improving the performance of coal-based solid waste filling material but also offers a new approach for realizing the resource utilization of coal mine waste. It provides theoretical support and technical backing for further understanding

and improvement in the promotion and application of fly ash backfill materials.

2 Experimental materials and preparation

2.1 Composition of raw materials

The fly ash filling material used in the test is composed of cement, fly ash, and crushed coal gangue, mixed according to a certain ratio. The fly ash was sourced from the Xingneng Power Plant of the Huadian Group, the coal gangue was obtained from the Xiaojihan Coal Mine in Yulin city, Shaanxi Province, and the cement was P.O.52.5 ordinary Portland cement produced by Zhucheng Yangchun Cement Co., Ltd. Ordinary tap water was used as the mixing water.

2.2 Characteristics of fly ash

The fly ash samples (FASs) were analyzed using an X-ray fluorescence spectrometer. The X-ray diffractometer (XRD) pattern is shown in [Figure 1a](#). The composition and content of the fly ash are provided in [Table 1](#). The experiment demonstrates that the reactivity of fly ash is determined by silicon, aluminum, and calcium oxide, and the higher their content, the greater the activity. The calcium oxide (CaO) in fly ash primarily acts as an active activator, promoting the pozzolanic reaction to form cementitious materials (e.g., calcium silicate hydrate, C–S–H), enhancing concrete strength and durability. It also regulates system alkalinity, but excessive CaO may induce volumetric expansion, requiring controlled dosage.

2.3 Cement

The specific surface area of the cement used in the experiments is 381 m²/kg, the apparent density is 3.16 g/cm³, and the standard consistency water consumption is 26.4%. The cement samples were analyzed using an X-ray fluorescence spectrometer, and the XRD pattern is shown in [Figure 1b](#). The composition and content of the composite Portland cement are provided in [Table 1](#).

2.4 Characteristics of coal gangue

The coal gangue used in the test is the raw gangue discharged from the underground (without calcination treatment), with a density of 2,550 kg/m³. After crushing using a hammer crusher, the particle size is less than 25 mm, with particles smaller than 5 mm accounting for 50%, 5–10 mm for 35%, and 10–25 mm for 15%. [Figure 1c](#) represents the test results of coal gangue mineral composition using a Rigaku D/Max 2500 X-ray Diffractometer. The ultraviolet-visible spectrophotometer (UV–VIS) and inductively coupled X-ray fluorescence spectrometer were used to test the chemical composition of coal gangue. According to the content classification of the chemical composition of coal gangue, the test coal gangue belongs to clay rock gangue.

2.5 Specimen production

Based on the accumulation of early physical and mechanical characteristic tests of fly ash filling materials in the early stage, the cement: fly ash: coal gangue ratio of 1:3:5, water–binder ratio of 0.63, and mass concentration of 78% were selected as the control group. Considering the influence of cement and fly ash content on the early-age hydration process of materials and their physical and mechanical properties, the experiment was divided into two parts, as shown in [Table 3](#). Through orthogonal experiments, the physical and mechanical properties of the water–binder ratio, the fly ash content, and filling materials were tested, respectively, with a total of five experimental groups. For each group, three cylindrical specimens were prepared, ensuring no fewer than three specimens under the same conditions. The fly ash samples were labeled FAS-1 to FAS-5. Specimen numbers FAS-1, FAS-2, and FAS-3 are correspond to a cement: fly ash: coal gangue ratio of = 1:3:5, with water–binder ratios is 0.56, 0.75, and 0.63, respectively; specimen numbers FAS-3, FAS-4, and FAS-5 were used to study the effect of the fly ash content, where, under a constant water–binder ratio of 0.63, fly ash accounted for 25%, 50%, and 75% of the total mass of cementitious materials, respectively. According to the ratio provided in [Table 2](#), the raw materials are weighed, and the materials are mixed. The newly mixed material was quickly loaded into a mold with a size of Φ50 mm × 100 mm and vibrated to the surface, and the surface of the slurry sample was sealed with a plastic bag to prevent water evaporation. According to China's technical specification for coal mine gangue-based solid waste filling (NB/T 11432-2023), curing should be carried out at a temperature of (20 ± 2)°C and a humidity of 80%.

2.6 Experimental system

The JWBK static volumetric porosity tester produced by Beijing Jingwei Gaobo Science and Technology Co., Ltd. was used to test the porosity of three types of samples at 12, 24, 36, and 48 h of hydration. According to the “Standard for Testing Methods of Mechanical Properties of Ordinary Concrete,” the MTS laboratory equipment NYL-2000 microcomputer-controlled electro-hydraulic servo-universal testing machine of Xi'an University of Science and Technology can accurately control the experimental process and automatically measure parameters such as stress and strain. The research results ([Liu et al., 2020](#); [Liang and Wei, 2016](#); [Shao et al., 2022a](#)) can ensure the reliability of the test results. The test system is shown in [Figure 2](#). First, fly ash materials are obtained using fly ash production equipment. Then, the microscopic characteristics of the material are obtained using the mineral composition testing system and the porosity testing system. Finally, the mechanical parameters of the material sample are obtained using the pressure testing system. The uniaxial compressive strength and elastic modulus of the samples were measured every 4 h for 12–48 h.

Under low-temperature conditions (such as in liquid nitrogen or liquid argon), in a sealed vacuum system, by changing the pressure of the adsorbate gas and using high-precision pressure sensors to measure the pressure changes before and after the adsorption of gas molecules by the sample, the amount of gas adsorption can be calculated, the isothermal adsorption–desorption curves can be depicted, and various physical analysis models

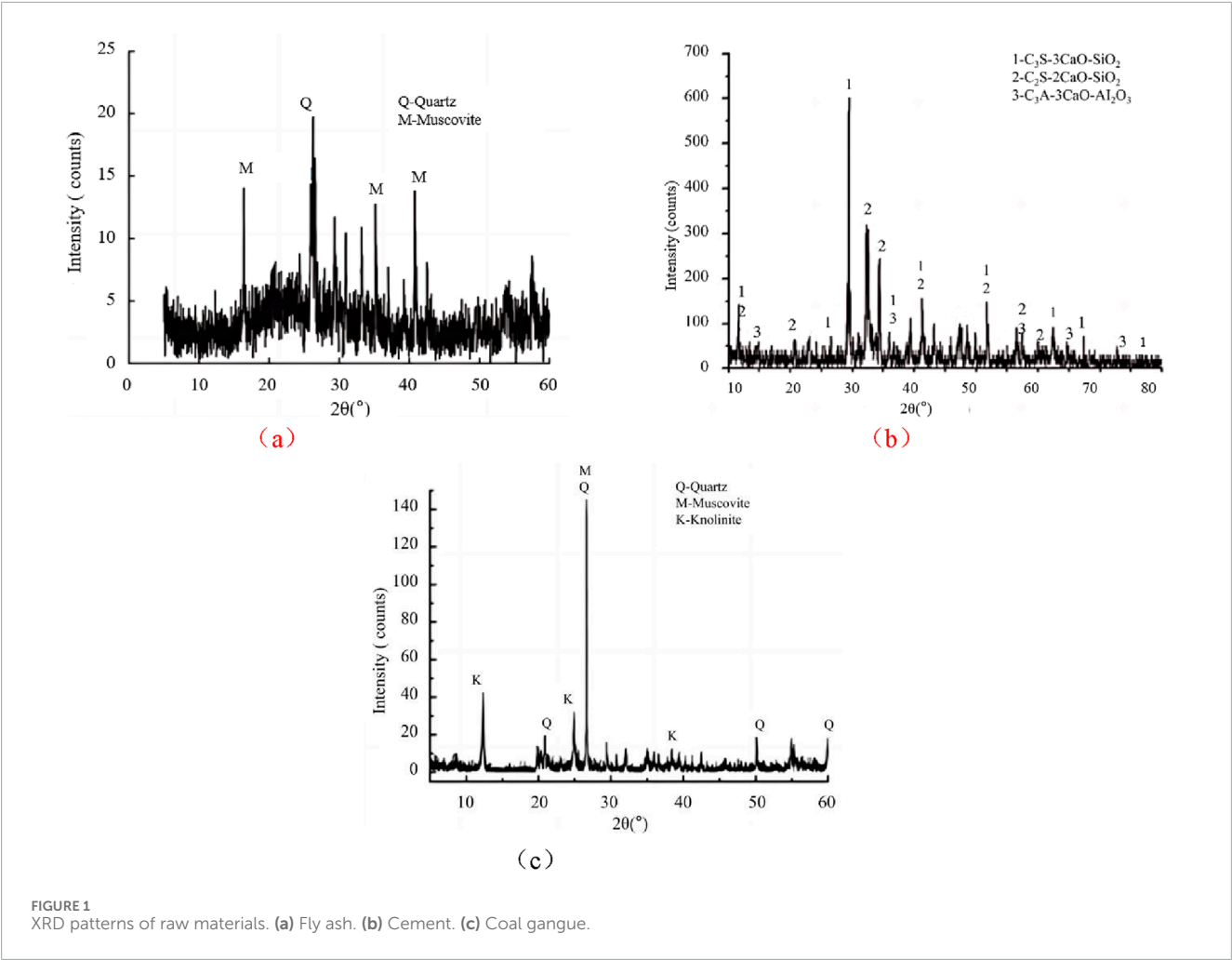


TABLE 1 Chemical composition and content of filling materials.

Composition	SiO ₂	Al ₂ O ₃	Fe ₂ O ₃	CaO	K ₂ O	TiO ₂	MgO	Na ₂ O	SO ₃	P ₂ O ₅	MnO	LOI
Fly ash	53.96	31.14	4.16	4.01	2.03	1.13	1.01	0.88	0.72	0.67	-	-
Cement	20.86	5.90	3.61	56.77	1.25	0.06	3.50	0.05	2.43	0.05	0.06	-
Coal gangue	49.69	23.44	5.42	4.02	1.79	0.89	0.81	0.35	0.16	0.18	0.11	13.14

TABLE 2 Material mixing ratio of samples.

Sample number	Cement: fly ash: coal gangue	Water–binder ratio	Explanation
FAS-1	1:3:5	0.56	Test of different water–binder ratio
FAS-2	1:3:5	0.75	
FAS-3	1:3:5	0.63	Control group
FAS-4	2:2:5	0.63	Test on different fly ash content
FAS-5	3:1:5	0.63	

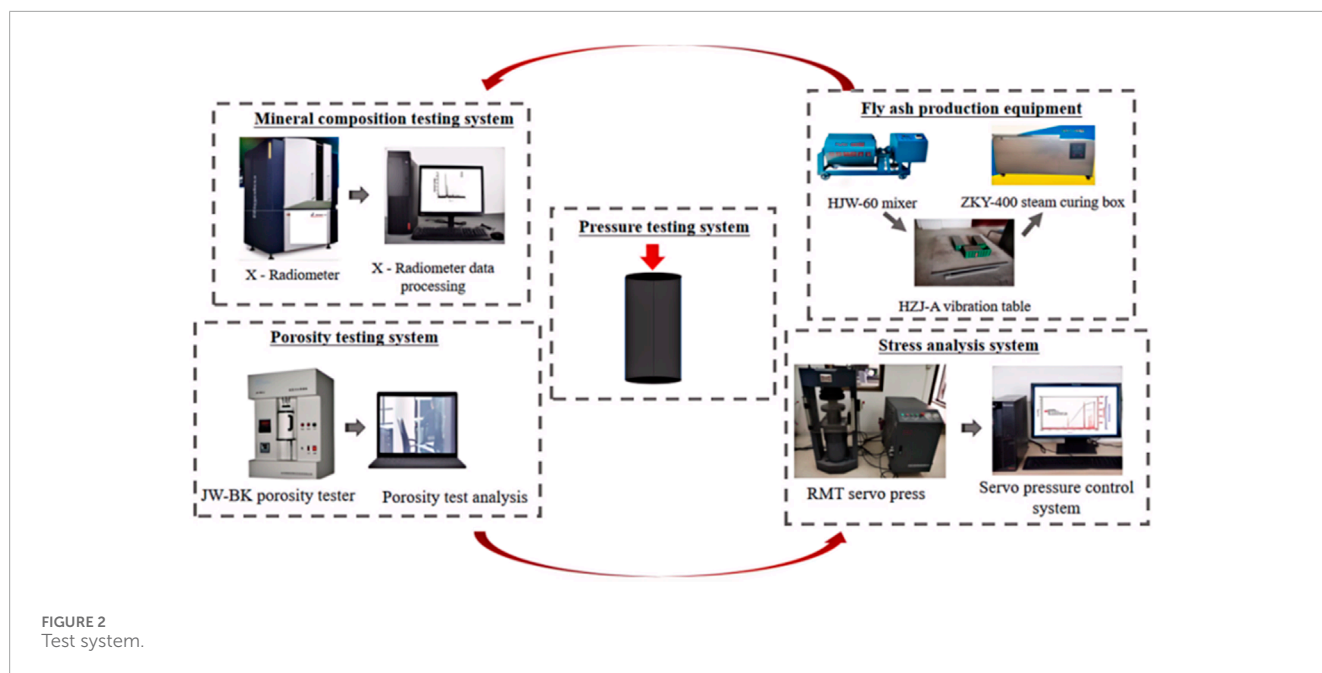


FIGURE 2
Test system.

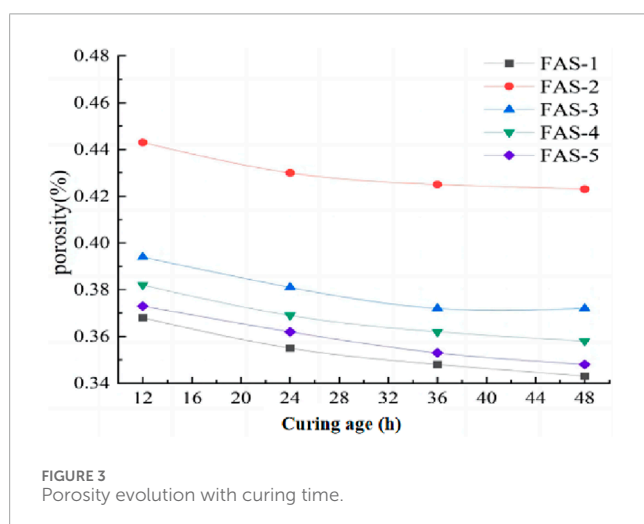


FIGURE 3
Porosity evolution with curing time.

can be applied for the analysis of specific surface area and pore volume.

3 Test results and analysis

3.1 Porosity test results

Using a pore analysis device, the time-dependent variation law of the pore volume of different filling materials was measured. The average values of porosity tests conducted on 20 samples with five different proportions at early ages of 12, 24, 36, and 48 h are plotted in Figure 3.

The hydration reaction between cement and fly ash is reflected in the physical properties of the specimens, specifically in the filling of the internal pore structure. As shown in Figure 3, at the same

time point, the smaller the water–binder ratio and the lower the fly ash content in different specimens, the smaller the porosity and the better the compactness of the specimens. The porosity of fly ash specimens exhibited a decreasing trend, and the rate of porosity reduction decreased as time increased. The reasons for this can be analyzed as follows:

- (1) Filling effect: As the hydration reaction progresses, newly generated hydration products gradually fill the pores inside the specimens, resulting in a decrease in porosity.
- (2) Impact of the fly ash content: The greater the fly ash content, the more filling particles it provides, and the more obvious the filling effect is, potentially resulting in a relatively faster rate of porosity reduction. However, excessive fly ash content may lead to unstable hydration products, requiring the control of an appropriate content.
- (3) Impact of the water–binder ratio: A smaller water–binder ratio means a relatively increased amount of cementitious material and an increased number of cement particles undergoing hydration reactions with water. This increases the cementitious hydration products within the concrete, further filling the pores and reducing porosity.

3.2 Effect of the water–binder ratio on compressive strength and elastic modulus characteristics

The uniaxial compressive strength and elastic modulus of fly ash filling material are the comprehensive reflection of the material's hydration degree and mechanical properties. Based on the ratio of cement: fly ash: coal gangue = 1:3:5, the relationship between uniaxial compressive strength, elastic modulus, and the water–binder ratio of samples with different water–binder ratios was

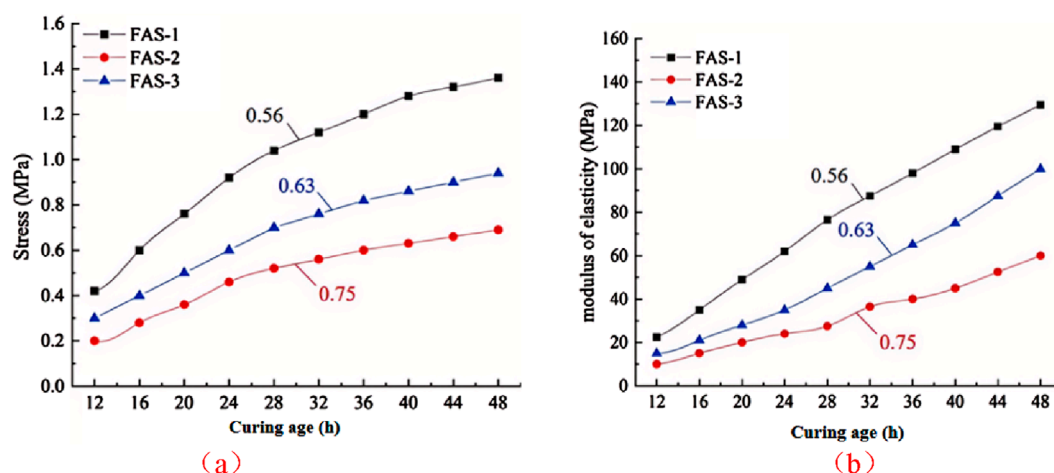


FIGURE 4 Relationship between uniaxial compressive strength, elastic modulus, and the water–binder ratio. (a) Uniaxial compressive strength; (b) modulus of elasticity.

analyzed, with the water–binder ratio as a variable. The relationship curve is shown in Figure 4.

As shown in Figures 4a, b, the uniaxial compressive strength and elastic modulus of the fly ash filling material specimens at an early age increase with time, indicating that the hydration reaction of fly ash is vigorous at this stage and the large amount of material generated through the reaction is helpful for early setting and increasing the strength of the specimen. However, as the water–binder ratio increases, the uniaxial compressive strength and elastic modulus of the specimens decrease significantly, indicating that the water–binder ratio has a significant effect on the hydration reaction, compactness, and strength of fly ash materials—an excessively high water–binder ratio inhibits the early-age strength development of fly ash. The results of Figure 4a show that the 48-hour strength of fly ash specimens is 1.36 MPa, 0.69 MPa, and 0.94 MPa, which indicates that the early-age strength of fly ash specimens with cement: fly ash: coal gangue = 1: 3: 5 is low, and the low early-age strength as filling material will affect the normal mining of the coal mine working face.

3.3 Effect of the fly ash content on compressive strength and elastic modulus characteristics

The above research shows that the early-age strength of fly ash specimens with cement: fly ash: gangue = 1: 3: 5 is lower. Therefore, by changing the ratio of fly ash to cement, the relationship between the fly ash content and early-age strength of specimens was studied, and the variation curves of uniaxial compressive strength and elastic modulus over time for specimens with different fly ash contents were obtained (Figure 5).

Uniaxial compressive strength and elastic modulus are both important parameters reflecting the mechanical properties of materials. In filling materials, as the hydration reaction progresses, the microstructure of the material changes, thereby affecting its

mechanical properties. Since the impact of the fly ash content on the hydration reaction rate and products is consistent, the uniaxial compressive strength and elastic modulus will be similarly affected, demonstrating similar curve trends. The uniaxial compressive strength and elastic modulus of specimens at an early age increase over time. However, with an increase in the fly ash content, the uniaxial compressive strength and elastic modulus of specimens at various time periods significantly decrease. In particular, when the fly ash content reaches 25%, there is a notable increase in uniaxial compressive strength and elastic modulus, indicating that the fly ash content significantly affects the hydration rate of the filling material, resulting in a reduction in the generated gel and hydraulic products of the filling material.

The hydration of cement in the early stage is gradually accelerated. Since the reference sample has begun to harden and become dense, the gradual decrease in porosity will make the cement paste mixed with fly ash become the main reason for the slow hydration reaction due to its adsorption and dispersion (inducing the continuous hydration of cement) and the channel or delayed hardening structure that has not been closed by hydration products.

The physical and chemical effects of fly ash include the micro-aggregate effect, dispersion effect, filling effect, and pozzolanic effect (Xu HC. et al., 2022). The dispersion effect and filling effect in the early hydration process are fully exerted, and no obvious pozzolanic activity is shown. Since the dispersion effect of fly ash will reduce the hydration rate of cement as a whole after replacing cement with fly ash in equal amounts, the initial activity of the material is relatively low. Although the hydration rate of the cement clinker will be accelerated, the overall hydration rate will be reduced, and the hydration products will be reduced. In addition, fly ash shows a filling effect at early stages, which changes pore connectivity and the ion transport pathways; this effect reduces pore connectivity, increases the length of the ion movement pathway, slows the hydration reaction rate, and becomes more pronounced as the fly ash content increases. The early hydration reaction of cement gradually accelerates. Since the reference sample has begun

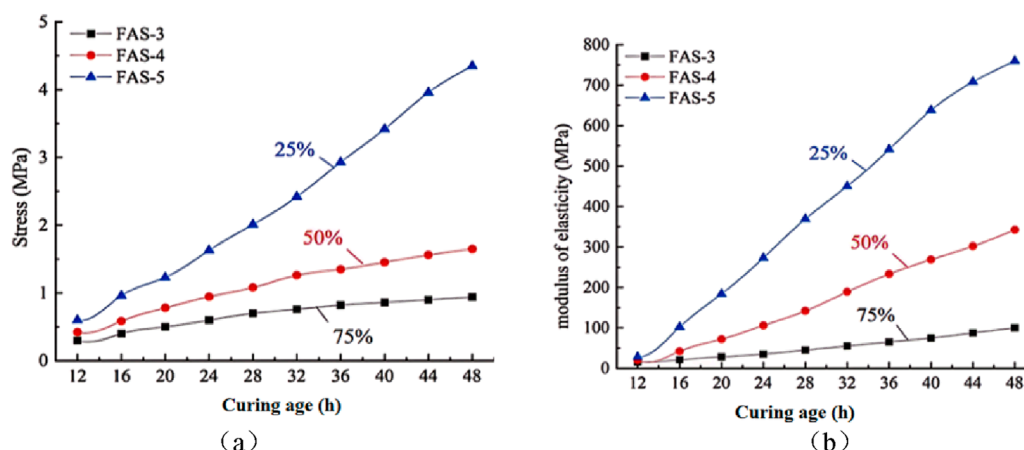


FIGURE 5 Relationship between uniaxial compressive strength, elastic modulus, and fly ash content; (a) uniaxial compressive strength; (b) modulus of elasticity.

to harden and become dense, the gradual reduction in porosity will cause the slurry to adsorb and disperse (inducing the continuous hydration of cement). The material that has not yet undergone the hydration reaction will block the channel or delay the formation of hardened structure, resulting in a slow early hydration reaction. Therefore, the early strength of the filling material is directly related to the content of fly ash; in other words, the early strength of the filling material is mainly determined through the cement hydration reaction. In order to improve the early strength of filling materials and avoid delaying coal mining time due to low strength, considering the ratio test, filling technology, and economic cost, it is determined to increase the early strength by reducing the content of fly ash.

As shown in Figure 5, when the fly ash content is 25%, the uniaxial compressive strength and elastic modulus exhibit a significant improvement. This may be because, under a specific mix ratio, the filling effect and micro-aggregate effect of fly ash are well utilized, resulting in a more compact microstructure of the material and thus enhancing its mechanical properties. On the other hand, 25% fly ash content may represent a balance point where the dispersion effect and filling effect of the material reach an optimal state, leading to improved stress and elastic values. However, this does not mean that a higher fly ash content is always better as excessive fly ash may lead to a reduction in hydration products, thereby degrading the material's mechanical properties.

3.4 Verification of the optimized proportion

To quickly improve the early strength of the filling material, the FAS-6 scheme of cement: fly ash: coal gangue = 2: 2: 5 is determined; the water-binder ratio is set to 0.63 as the benchmark, and according to the relevant research results (Xu H. et al., 2022; Shao et al., 2022b; Shao et al., 2022c), early-strength water-reducing agents, accelerators, expansion agents, and other additives are added as the optimal ratio of filling material, and finally, the optimal ratio test is carried out. The specific configuration is shown in Table 3.

Comparing the mechanical properties of filling materials with different proportions in Figures 5, 6, it can be observed that after the fly ash content is reduced from 75% to 50%, the 48-h strength and elastic modulus of the specimens are increased by 1.74 times and 2.88 times, respectively. After adding admixtures, the 48-h uniaxial compressive strength and elastic modulus of the specimens were 1.36 MPa and 3.16 MPa, respectively, which were 1.76 times and 2.36 times higher than those without additives. It shows that reducing the amount of fly ash and adding admixtures can not only strengthen the hydration reaction ability of cementitious materials and improve the working performance of paste materials but also improve the problem of roof contact in the later stage of fly ash filling materials. For example, an early-strength water-reducing agent can improve the fluidity and early strength of the material; an accelerator can effectively adjust the setting time of the material, and the expansion agent contributes to the later-stage expansion at the top.

4 Discussion

Xiang (2004) showed that the spherical shape of fly ash particles reduces both yield stress and apparent viscosity. Fly ash particles exhibit irregular porous morphologies with complex surface textures, which enhance their water adsorption capacity through both surface interactions and internal pore retention. This dual water-binding mechanism reduces the availability of free water required for maintaining slurry fluidity. This is an important factor to reduce the fluidity of filling material slurry under the same water cement ratio. Compared with the large amount of fly ash, reducing the content of fly ash reduces the rough surface area of adsorbed free water, which can effectively release the pore water filled between the pores of cement particles. Therefore, when fly ash particles are added to cement, the rough surface of the particles even increases the friction between the particles inside the paste. Based on the above analysis, we can know that the shape and surface roughness of fly ash have a negative impact on the rheology of the filling material system. Therefore, when the content of fly ash particles is slightly higher, the

TABLE 3 Verification of the optimized proportion of fly ash filling materials.

Sample number	Cement: fly ash: coal gangue	Water–binder ratio	Admixture (%)		
			Early-strength water-reducing agent	Accelerator	Swelling agent
FAS-3-2	1:3:5	0.63	1.5	3	5.5
FAS-6	2:2:5	0.63			

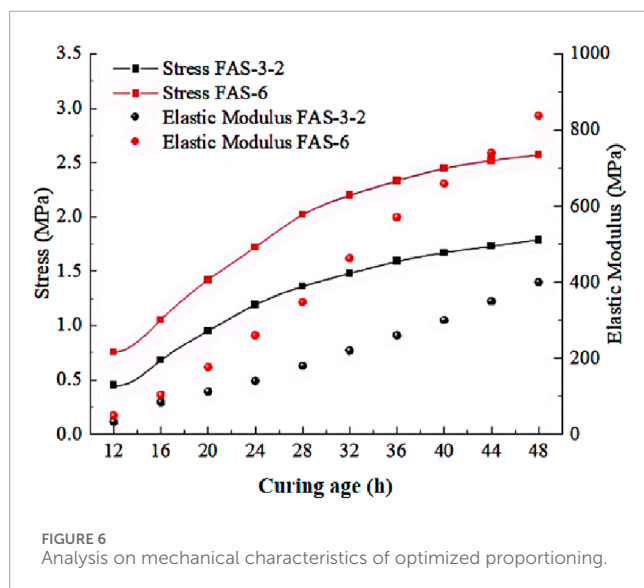


FIGURE 6 Analysis on mechanical characteristics of optimized proportioning.

rheological properties of the material are worse than those of pure cement slurry.

To provide a more intuitive representation of the hydration products of filling materials, an SEM device model TM4000Plus II produced by Hitachi of Japan was used to observe the microscopic morphology of hardened cement paste. This device can clearly characterize the compactness of the hardened paste structure, the degree of particle hydration, and the morphological characteristics of the hydration products. The morphologies of the hydration products of filling materials with different fly ash contents are shown in Figure 7.

For the product morphology of the fly ash cement system with a hydration age of 48 h, as shown in Figure 7a, it can be observed that the hydration products of the 50% fly ash content filling material system are fewer, and the unhydrated fly ash particles can be clearly observed. Only part of the particle surface is eroded, and the needle-shaped AFt (trisulfide-type hydrated calcium sulfoaluminate) is embedded in the large particle gap. The higher sulfur content promotes the formation of more ettringite; the overall structure of the hydration product is loose, and the degree of hydration is low. From the SEM image of Figure 7b, a large number of fine fibrous C–S–H gels are observed in a clustered needle-like shape and overlapping with CH to form a more stable structure, indicating that the early hydration degree of 50% fly ash content is higher, which is consistent with the reference Guo et al. (2014). When the

fly ash content is low (<30%), the addition of HVFAC is beneficial in accelerating the hydration process of the system. On this basis, we analyze the underlying reasons through the hydration reaction process. For example, the hydration components of regions I and II in Figures 7c,d are mainly composed of Ca, Si, O, and other elements. It can be basically confirmed that the composition is the C–S–H gel. Among them, the cluster needle-shaped C–S–H gel in Region-I is more abundant, which can be attributed to the cement hydration reaction (Pan et al., 2019; Guo et al., 2014; Kwan and Li, 2013). The cluster needle-shaped C–S–H gel in Region-II is less abundant, and the surface is rough. Unhydrated fly ash particles can clearly visible, indicating that this region corresponds to be the hydration reaction of fly ash. Some scholars mostly studied the individual effect of the rod-like substances without considering the effect of clustered acicular C–S–H gels on the early strength of fly ash. The effect of cluster needle C–S–H gels on the early strength of fly ash was not considered. The analysis of hydration product Region-III (Figure 7e) confirms that it is AFt, and Region-IV (Figure 7f) is mainly CH. In Figure 7a, a large amount of coarse fibrous C–S–H is formed in the hydration products, which is overlapped with CH, and there are fewer pores. It is observed that the original fly ash particles are less, indicating that the hydration degree of the filling material with 50% fly ash content is higher.

The reason is that when the cement with 75% fly ash is hydrated for 48 h, there are fewer hardening products, and unhydrated fly ash particles are clearly visible. Only the surface of some particles is eroded, and more needle-like AFt is formed in the gap between the large particles and hydration products. The dissolution of anhydrite in fly ash results in a higher concentration of SO_4^{2-} around the particles, and more AFt is formed in the gap of the particles. Due to the rapid dissolution of $\text{CaSO}_4 \cdot 2\text{H}_2\text{O}$, AFt is formed with the calcium and aluminum components in the material. From CaSO_4 on the surface of the fly ash particles to $\text{CaSO}_4 \cdot 2\text{H}_2\text{O}$, there is an expansion, and $\text{CaSO}_4 \cdot 2\text{H}_2\text{O}$ is rapidly dissolved to precipitate SO_4^{2-} . Combined with the calcium and aluminum components in the liquid phase, AFt is formed, and the second volume expansion occurs. The volume expansion makes the material dense, which is beneficial to the early-age strength of the material. Some scholars have analyzed the hydration reaction of fly ash but did not explain the volume expansion in the chemical reaction of the material, especially the two expansions formed by the two reactions. Compared with the 75% fly ash content, the number of AFt formed in the 50% fly ash content material at 48 h hydration is significantly reduced, as observed in the SEM image of Figure 7a,b. This is because 50% fly ash content cement has more cement content,

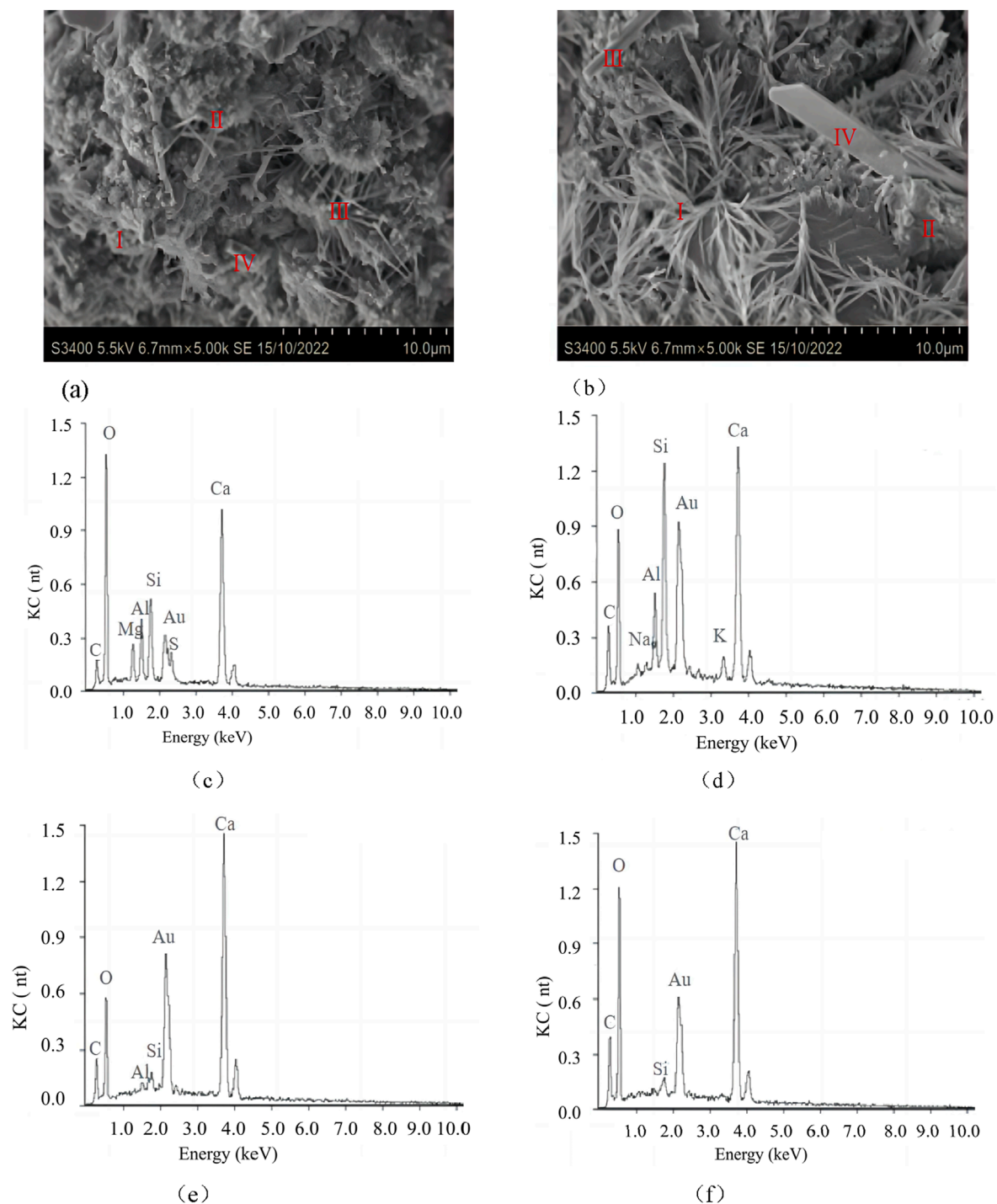


FIGURE 7 Morphology and energy spectrum of 48-h hydration products of filling materials with different fly ash contents. **(a)** 75% fly ash content filling materials. **(b)** 50% fly ash content filling materials. **(c)** Region-I. **(d)** Region-II. **(e)** Region-III. **(f)** Region-IV.

a faster dissolution rate, a faster hydration rate, and more hydration products, and because of the filling effect of fly ash, the structure of hydration products is more compact. The dissolution rate of SO_4^{2-} in 50% fly ash content cement is faster; Aft is formed earlier and partially covered by hydration products. There are more plate-like CHs in the hydration products of cement with 50% fly ash content for

48 h. At this time, it is mainly CH produced by clinker hydration and CH converted by free calcium oxide in water, while the hydration degree of the specimen with 75% fly ash content is low, and CH consumption is minimal.

With a decrease in the fly ash content and an increase in the water-to-binder ratio, the uniaxial compressive strength and elastic

modulus of materials decrease. However, the empirical formula of the relationship between the water-to-binder ratio, curing age, and compressive strength of materials obtained from Saavedra et al. (2016) is explained through experiments. In the studies by Saavedra and Gutiérrez (2017), Zhang (2020), Maenami et al. (2004), and Mahmoodzadeh and Chidiac (2013), the typical fly ash of Japanese and European pressurized fluidized bed combustion systems was characterized through electron microscopy and energy-dispersive X-ray spectroscopy. It was analyzed that the pozzolanic reaction in the hydration process was relatively small, while the reaction of cement hydration to form gel material had always played a major role and generated a large amount of $\text{Ca}(\text{OH})_2$. This study not only obtained the relationship between different curing times, fly ash content, and compressive strength of the material but also compared and analyzed the hydration reaction process of 75% and 50% fly ash from the concentration of SO_4^{2-} , the formation of Aft, and the consumption of CH in the hydration reaction process. The microstructure changes in coal during the reaction process reveal the hydration reaction process and consolidation mechanism of high-volume filling materials.

In general, with the decrease in fly ash parameters, more hydration products are generated by the hardened slurry of the filling material, fewer pores are formed, and the slurry structure becomes denser, which is greatly improved compared with the microstructure of 75% fly ash. The relationship between the ratio parameters, such as the water-to-binder ratio and fly ash content, and the internal structure of the filling material and the mechanical properties at the early age is studied. It can be used to solve the selection of filling materials in different regions during the filling mining process of coal mines. The formation of the filling body structure (for example, to meet the formation of the filling result, in the case of long consolidation time, the material with low early-age strength is selected, and the material with high early-age strength is selected to affect the normal mining of coal), reducing the influence of filling consolidation on coal mining, is of great significance and practical value.

5 Conclusion

- (1) When the fly ash content is reduced from 75% to 50%, the 48-h uniaxial compressive strength and elastic modulus of the filling material increase by 3.06 times and 6.80 times, respectively. This indicates that as the fly ash content decreases, the hydration products generated by the hardened paste of the filling material increase, the pores decrease, and the structural density of the paste increases.
- (2) The early-age hydration reaction and mechanical properties of fly ash filling materials are dominated by cement. The dispersing and filling effects of fly ash during the hydration process are fully exerted, but it does not exhibit significant pozzolanic activity. Therefore, it is proposed to reduce the water-to-binder ratio and fly ash content while adding admixtures to improve the early-age strength of the material.
- (3) A filling material with a water-to-binder ratio of 0.63 and a fly ash content of 50% has a high hydration rate, high compactness, and high early-age strength, making it more suitable for coal mine filling.
- (4) This article studies the early-age physical and mechanical properties and hydration reactions of fly ash and gangue filling materials, revealing the hydration reaction process and consolidation mechanism of large-volume filling materials. However, due to the limitations of experimental conditions, real-time monitoring of the evolution of material hydration products using physical detection methods was not possible. Therefore, we will further investigate the relationship between large volumes of fly ash materials and their mechanical properties through changes in bulk resistivity during the hydration reaction process. Based on the physical and mechanical properties of filling materials with different fly ash contents, we designed a reasonable filling method to provide a scientific basis for safe and green mining in coal mines.

Data availability statement

The datasets presented in this study can be found in online repositories. The names of the repository/repositories and accession number(s) can be found in the article/supplementary material.

Author contributions

ZW: Writing – original draft, Data curation. LX: Writing – review and editing, Methodology. CX: Visualization, Writing – original draft. WZ: Methodology, Writing – review and editing.

Funding

The author(s) declare that no financial support was received for the research and/or publication of this article.

Conflict of interest

The authors declare that the research was conducted in the absence of any commercial or financial relationships that could be construed as a potential conflict of interest.

Generative AI statement

The author(s) declare that no Generative AI was used in the creation of this manuscript.

Publisher's note

All claims expressed in this article are solely those of the authors and do not necessarily represent those of their affiliated organizations, or those of the publisher, the editors and the reviewers. Any product that may be evaluated in this article, or claim that may be made by its manufacturer, is not guaranteed or endorsed by the publisher.

References

- Charpin, L., Lepape, Y., Coustabeau, É., Toppani, É., Heinfling, G., Le Bellego, C., et al. (2018). A 12 year EDF study of concrete creep under uniaxial and biaxial loading. *Cem. Concr. Res.* 103, 140–159. doi:10.1016/j.cemconres.2017.10.009
- Chen, S., Wu, C., and Yan, D. (2019). Binder-scale creep behavior of metakaolin-based geopolymer. *Cem. Concr. Res.* 124, 105810. doi:10.1016/j.cemconres.2019.105810
- Guo, W. Z., Jin, Y. F., and Li, H. T. (2014). Effects of additives on properties of high volume fly ash slurry. *Coal Technol.* 33 (11), 7–10. doi:10.13301/j.cnki.ct.2014.11.003
- Huynh, T., Hwang, C., and Limongan, A. (2018). The longterm creep and shrinkage behaviors of green concrete designed for bridge girder using a densified mixture design algorithm. *Cem. Concr. Compos.* 87, 79–88. doi:10.1016/j.cemconcomp.2017.12.004
- Jiang, L. (2020). Comprehensive utilization situation of fly ash in coal-fired power plants and its development suggestions. *Clean. Coal Technology* 26 (4), 31–39. doi:10.13226/j.issn.1006-6772.F19062501
- Kwan, A. K. H., and Li, Y. (2013). Effects of fly ash microsphere on rheology, adhesiveness and strength of mortar. *Constr. And Build. Mater.* 42, 137–145. doi:10.1016/j.conbuildmat.2013.01.015
- Lai, X. P., Zhang, S., Cao, J. T., Sun, Y., and Xin, F. (2025). Difference of “whole-process and stages” response law of energy evolution regulated by high energy storage rock modification. *Geohazard Mechanics* 3, 99–108. doi:10.1016/j.ghm.2025.06.001
- Lavergne, F., and BartheLeMY, J. (2020). Confronting a refined multiscale estimate for the aging basic creep of concrete with a comprehensive experimental database. *Cem. Concr. Res.* 136, 106163. doi:10.1016/j.cemconres.2020.106163
- Li, J. Y., and Wang, J. M. (2019). Comprehensive utilization and environmental risks of coal gangue: a review. *J. Clean. Prod.* 239, 117946. doi:10.1016/j.jclepro.2019.117946
- Liang, L., Zhang, X., and Liu, Q. L. (2023). The influence of pasterheological properties on the properties of ultrahigh ductility cement based materials. *Introd. Mater.* (5), 1–11.
- Liang, S. M., and Wei, Y. (2016). Influence of microstructure on micro creep and mechanical properties of hardened cement paste. *J. Chin. Ceram. Soc.* 44 (02), 181–188. doi:10.14062/j.issn.0454-5648.2016.02.01
- Liu, Q. Y., Li, H. C., Peng, Y. J., and Dong, X. B. (2020). Nanomechanical properties of multi-wall carbon nanotubes/cementitious composites. *Acta Mater. Compos. Sin.* 37 (04), 952–961. doi:10.13801/j.cnki.fhclxb.20190730.004
- Maenami, H., Isu, N., Ishida, E. H., and Mitsuda, T. (2004). Electron microscopy and phase analysis of fly ash from pressurized fluidized bed combustion. *Cem. And Concr. Res.* 34 (5), 781–788. doi:10.1016/j.cemconres.2003.08.011
- Mahmoodzadeh, F., and Chidiac, S. E. (2013). Rheological models for predicting plastic viscosity and yield stress of fresh concrete. *Cem. And Concr. Res.* 49, 1–9. doi:10.1016/j.cemconres.2013.03.004
- Mallick, S., Anoop, M., and Rao, K. (2019). Creep of cement paste containing fly ash an investigation using microindentation technique. *Cem. Concr. Res.* 121, 21–36. doi:10.1016/j.cemconres.2019.04.006
- Ni, T. Y. (2020). *Tensile creep characteristics and its evaluation of high strength concrete containing mineral admixtures at early ages*. Hangzhou: Zhejiang University of Technology.
- Pan, G., Li, P. C., Chen, L. J., and Liu, G. (2019). A study of the effect of rheological properties of fresh concrete on shotcrete rebound based on different additive components. *Constr. Build. Mater.* 224, 1069–1080. doi:10.1016/j.conbuildmat.2019.07.060
- Park, B., and Choi, Y. (2021). Hydration and pore-structure characteristics of high-volume fly ash cement pastes. *Constr. Build. Mater.* 278, 122390. doi:10.1016/j.conbuildmat.2021.122390
- Peng, S. P., and Bi, Y. L. (2020). Strategic consideration and core tech nology about environmental ecological restoration in coal mine areas in the yellow river basin of China. *J. China Coal Soc.* 45 (4), 1211–1221.
- Qiu, J. D., Huang, R., Wang, H. W., Wang, F., and Zhou, C. T. (2025). Rate-dependent tensile behaviors of jointed rock masses considering geological conditions using a combined BPM-DFN model: strength, fragmentation and failure modes. *Soil Dyn. Earthq. Eng.* 195, 109393. doi:10.1016/j.soildyn.2025.109393
- Saavedra, W. G., Angulo, D. E., and Gutierrez, R. M. D. (2016). Fly ash slag geopolymer concrete: resistance to sodium and magnesium sulfate attack. *J. Mater. Civ. Eng.* 28 (12), 04016148. doi:10.1061/(asce)mt.1943-5533.0001618
- Saavedra, W. G., and Gutiérrez, R. M. (2017). Performance of geopolymer concrete composed of fly ash after exposure to elevated temperatures. *Constr. Build. Mater.* 154, 229–235. doi:10.1016/j.conbuildmat.2017.07.208
- Shao, Y. W., Suo, Y. L., and Xiao, J. (2022a). Creep characteristic test and creep model of frozen soil. *Sustainability* 14. doi:10.3390/su15053984
- Shao, Y. W., Suo, Y. L., Xiao, J., Bai, Y., Yang, T., and Fan, S. (2022c). Dynamic evolution characteristics of oil gas coupling fractures and dynamic disaster of coal mass in coal and oil resources costorage areas. *Appl. Sci.* 12, 4499. doi:10.3390/app12094499
- Shao, Y. W., Suo, Y. L., and Yang, T. (2022b). Mechanism of loading fracture of coal mass and formation of oil and gas disaster channel in coal and oil resources costorage area. *Shock Vib.*, 3372793. doi:10.1155/2022/3372793
- Sohan, B. S., Noah, H., and Seyed, A. (2023). Coal-based graphene oxide-like materials: a comprehensive review. *Carbon* 215, 118447. doi:10.1016/j.carbon.2023.118447
- Wyrzykowski, M., Scrivener, K., and Lura, P. (2019). Basic creep of cement paste at early age - the role of cement hydration. *Cem. Concr. Res.* 116, 191–201. doi:10.1016/j.cemconres.2018.11.013
- Xiang, Y. (2004). *The basic properties of coal shales and basic study on using coal shales as the filler of rubber*. Taiyuan: Taiyuan University of Technology.
- Xu, H. C., Lai, X. P., Zhang, S., Shan, P., Wu, Z., Xu, H. D., et al. (2022b). Precursor information recognition of rockburst in the coal-rock mass of meizoseismal area based on multiplex microseismic information fusion and its application: a case study of wudong coal mine. *Lithosphere* 2022. doi:10.2113/2022/7349759
- Xu, H. C., Lai, X. P., Shan, P. F., Yang, Y. B., Zhang, S., Yan, B. X., et al. (2022a). Energy dissimulation characteristics and shock mechanism of coal-rock mass induced in steeply-inclined mining: comparison based on physical simulation and numerical calculation. *Acta Geotech.* 11, 9. doi:10.1007/s11440-022-01617-2
- Yang, B. G., Yang, J., Yu, Y., Li, D., Jiang, B., and Cheng, K. (2017). Proportioning test and hydration mechanism study of new cementitious filling materials in coal mines. *J. Min. Sci.* 2 (5), 475–481. doi:10.19606/j.cnki.jmst.2017.05.009
- Yang, K., Zhao, X. Y., He, X., Wei, Z., Zhang, J. Q., and Ji, J. S. (2021b). Experimental study on the ratio of coal-based solid waste filling materials. *Shanxi Coal* 41 (4), 2–6.
- Yang, K., Zhao, X. Y., He, X., and Wei, Z. (2022). Basic theory and technical system of green filling of multi source coal-based solidwaste. *J. China Coal Soc.* 47 (12), 4201–4216. doi:10.13225/j.cnki.jccs.2022.0899
- Yang, Y. X., Wang, K. Y., and Ren, L. (2021a). Evaluation and coupling coordination analysis of high quality development of China's coal industry: empirical research based on data from 2000 to 2019. *J. Min. Sci. Technol.* 6 (6), 764–776.
- Yao, J., Yao, S., Huang, S., Ni, T., Jiang, C., Yang, Y., et al. (2023). The influence of fly ash on the tensile creep prediction of high strength concrete at early ages. *Mater.* 16 (4), 1337. doi:10.3390/ma16041337
- Yu, Y. (2017). *Research and development of new cemented filling materials for coal mines and their performance*. Beijing: China University of Mining and Technology.
- Zhang, J. Q., Yang, K., He, X., Zhang, L., Wei, Z., Zhao, X., et al. (2023). Study on mechanical properties and damage characteristics of coal-based solid waste cemented backfill. *Constr. Build. Mater.* 368, 130373. doi:10.1016/j.conbuildmat.2023.130373
- Zhang, S., Sun, Y., Cao, J. T., Lai, X. P., and Wu, L. Q. (2025). Research and optimization on the strength recovery mechanism of post peak fragmentation grouting reinforcement in mining rock mass. *Frontiers in Materials.* 12. doi:10.3389/fmats.2025.1612050
- Zhang, X. Z. (2022). Effects of low calcium fly ash content, water binder ratio and curing age on compressive strength of concrete. *J. Nanyang Inst. Technol.* 14 (2), 76–81. doi:10.16827/j.cnki.41-1404/z.2022.02.013
- Zhou, C. T., Rui, Y. C., Qiu, J. D., Wang, Z., Zhou, T., Long, X., et al. (2025). The role of fracture in dynamic tensile responses of fractured rock mass: insight from a particle-based model. *Int. J. Coal Sci. and Technol.* 12, 39. doi:10.1007/s40789-025-00777-2
- Zhou, W. L., Sun, W., Chen, C. C., and Miao, C. W. (2011). Characterization for micro mechanical properties of cementitious materials by nanoindentation technique. *J. Southeast Univ. Nat. Sci. Ed.* 41 (02), 370–375.